Advances in Aircraft and Spacecraft Science, *Vol. 10, No. 1 (2023) 83-106*
https://doi.org/10.12989/aas.2023.10.1.083

Thermomechanical behavior of Macro and Nano FGM sandwich plates

Soumia Benguediab[1], Tayeb Kebir[2], Fatima Zohra Kettaf[3], Ahmed Amine Daikh*[2,4], Abdelouahed Tounsi[5], Mohamed Benguediab[6] and Mohamed A. Eltaher[7,8]

[1]Department of Civil Engineering and Hydraulic, Faculty of Technology, University of Saida, Algeria
[2]Department of Technical Sciences Center University Salhi Ahmed, Naâma 45000, Algeria
[3]Department of Mechanical Engineering, University of Sciences and Technology Mohamed Boudiaf Oran, Algeria
[4]Laboratoire d'Etude des Structures et de Mécanique des Matériaux, Département de Génie Civil, Faculté des Sciences et de la Technologie, Université Mustapha Stambouli, Mascara 29000, Algeria
[5]Laboratory of Materials and Hydrology, Faculty of Technology, University of Sidi Bel Abbes, Algeria
[6]Laboratory of Materials and Reactive Systems, Faculty of Technology, University of Sidi Bel Abbes, Algeria
[7]Faculty of Engineering, Mechanical Design and Production Dept, Zagazig University, Zagazig, Egypt
[8]Faculty of Engineering, Mechanical Engineering Department, King Abdulaziz University, Jeddah, P.O. Box80204, Saudi Arabia

(Received August 14, 2022, Revised January 21, 2023, Accepted January 25, 2023)

Abstract. In this work, the static behavior of FGM macro and nano-plates under thermomechanical loading. Equilibrium equations are determined by using virtual work principle and local and non-local theory. The novelty of the current model is using a new displacement field with four variables and a warping function considering the effect of shear. Through this analysis, the considered sandwich FGM macro and nanoplates are a homogeneous core and P-FGM faces, homogeneous faces and an E-FGM core and finally P-FGM faces and an E-FGM core. The analytical solution is obtained by using Navier method. The model is verified with previous published works by other models and very close results are obtained within maximum 1% deviation. The numerical results are performed to present the influence of the various parameters such as, geometric ratios, material index as well as the scale parameters are investigated. The present model can be applicable for sandwich FG plates used in nuclear, aero-space, marine, civil and mechanical applications.

Keywords: functionally graded material; local and nonlocal theory; nanoplate structure; new plate displacement field; sandwich structure; static analysis

1. Introduction

Functionally graded materials (FGMs) are a type of composite materials that have material properties change continuous with specific function between two surfaces without interruption, eliminating the phenomenon of stress concentration encountered in composite materials layers. Due to their lightness, high rigidity and energy absorption capacity, sandwich structures are

*Corresponding author, Ph.D., E-mail: aadaikh@cuniv-naama.dz

http://www.techno-press.org/?journal=aas&subpage=7 ISSN: 2287-528X (Print), 2287-5271 (Online)

increasingly used in various industries such as automotive, aerospace, civil engineering, and mechanical structures, aeronautics and nuclear, (Lindström and Hallström 2010, Dean *et al*. 2011, Sekkal *et al*. 2017a, Hamed *et al*. 2020, Eltaher and Mohamed 2020, Daikh *et al*. 2021, Ramteke *et al*. 2021a). Currently, sandwich nano/micro scale structures can be used of in various industries, such as nano-plates and nano-beams in nano-electro-mechanical (NEMS) and micro-electro-mechanical (MEMS) instruments, (Eltaher *et al.* 2018, Karamanli *et al.* 2023)).

It is necessary to understand the response of these nano/microstructures due to the scaling effect.We can find several types of sandwich structures. Often used structures are sandwich structures with homogeneous core and FGM faces, homogeneous faces and FGM core and finally FGM faces and FGM core (Librescu and Hause 2000). The gradation of FGM may be described by power function (P-FGM), exponential function (E-FGM), Sigmoid function (S-FGM), (Hamed *et al*. 2016, Eltaher *et al*. 2022, Attia *et al*. 2022).

The need to develop mathematical models to predict the response of FGM sandwich plates is due to the increasing use of FGM sandwich structures as a structural element. Various models have been developed based on plate theory have been developed to accurately study their bending, stability, and vibration behaviors. In general, these theories are classified into three categories: classical plate theory (CPT), first order shear strain theory (FSDT), and Higher Order Shear Deformation Theory (HSDT). The simplest theory is the classical plate theory (CPT) it is a theory which is based on the assumptions of Kirchoff (1850), it neglects the effect of the transverse shear strain, this theory gives precise results for thin plates (Javaheri and Eslami 2002). Reissner (1850) and Mindlin (1851) developed the First Order Shear Deformation Theory (FSDT) which accounts for the effect of transverse shear by means of a linear variation of the displacement in the plane through the thickness (Nuguyen *et al*. 2008, Zhao *et al.* 2009, Mantari 2015). This theory gives sufficiently precise results for thick and moderately thick plates but requires the determination of a shear correction factor. Many high order plate shear strain theories have been developed for to avoid the use of the shear correction factor, such as Reddy's third order plate shear strain theory (TSDT) (Reddy (1997)), the sinusoidal shear strain plate theory (SSDT) (Touratier 1991) and the exponential shear strain plate theory (ESDT) (Karama *et al.* 2003).

In recent years, several high order HSDT theories have been proposed to study the response of structural elements. Three categories of theories are defined as follow: high order theories without thickness stretch effect and theories with thickness stretch effect, these theories are called quasi 3-D theories. Reddy and Chen (2001) presented a 3D model for an FG plate subjected to applied mechanical and thermal loads. The bending behavior of sandwich plates subjected to mechanical loads using several HSDT theories, Xiang *et al.* (2009). Boussoula *et al*. (2020) investigated thermo mechanical analysis of the bending of sandwich plates made of a functional gradation material with a P-FGM face sheets and E-FGM and symmetrical S-FGM core using a shear strain theory of order n. Merdaci *et al.* (2011), Ameur *et al*. (2011), Abbas *et al*. (2020) developed a high order shear strain theory (HSDT) with four unknowns for FG sandwich plates and FG plates using the sinusoidal function with hypotheses similar to those of Shimpi (2009). This theory was used by Tounsi *et al.* (2013) for the analysis of the thermoelastic bending of sandwich plates and the bending response of FG plates under thermo mechanical loading Zidi *et al.* (2014). Otherresearchers (Ait Yahia *et al*. 2015, Mahi *et al*. 2015, Zine *et al*. 2018) have applied the refined theory of high order shear strain (HDST) for bending and free vibration analysis of plates isotropic, functionally graded, sandwich and laminated composites and have obtained precise results. A simple plate shear strain theory for the analysis of buckling, bending and free vibration of functionally graduated (FG) plates has been proposed by Bellifa *et al*. (2016, 2017a). Belabed *et*

al. (2018) presented a vibratory analysis of FG sandwich plates using a novel three-unknown hyperbolic shear strain theory. Chikh *et al.* (2017) analyzed thermal buckling using a simplified higher order shear strain theory (HSDT) for cross-ply laminated plates. Malhari *et al.* (2022) studied numerically by finite element method, the nonlinear vibration of multidirectional porous FG panel under thermal environment using HSDT. Effect of grading pattern and porosity on static bending, eigen characteristics and natural frequencies of porous functionally graded structures are presented by Ramteke *et al.* (2019, 2020a, b, 2021b, c). However, the nonlinear mechanical response of multi-directional functionally graded porous panels are investigated by Ramteke *et al.* (2022a-c). Melaibari *et al.* (2022, 2023) developed mathematical and physical analyses of middle/neutral surfaces formulations in studing static response of 2D FGM plates with movable/immovable boundary conditions. Mohamed *et al.* (2022). Assie *et al.* (2023) investigated the static bending analysis of 2D FG plate on the basis of unified higher order shear deformation plate theories.

The study of the mechanical behavior of plates of different geometries and sizes presents a great importance in the design.In addition to the theories developed concerning macrostructures, several investigations have been carried out on the study of behaviors of these nanostructures resulting from new class materials such as functional grade materials (FGM structures) whose material properties gradually vary and continuously in each direction. The results of the experimental simulation on these structures showed a significant effect of the size on the mechanical properties and consequently on the static and dynamic response of micro and nano structures.Several non-local theories taking into account the scale effect have been proposed: the strain gradient theory (Aifantis 1999), the micro-polar theory (Eringen 1967) and the non-local theory of elasticity (Eringen 1972). The influence of the size is taken into account by the introduction of the intrinsic scale length in the constitutive relations.Several authors have used the non-local model to predict the mechanical responses of nanostructures (Zenkour and Abouelregal 2015, Li *et al.* 2016a, Besseghier *et al.* 2015, Abdelrahman *et al.* 2021a, b, c, Alazwari *et al.* 2022a, b, Esen *et al.* 2021, 2022a, b, Hendi *et al.* 2021). A dynamic and static analysis of macro and nano FGM plates was presented by Dastjerdi *et al.* (2017) using an exact three-dimensional elasticity considering thermal effects. A study of the characteristics of free vibration of FG plates at the nanoscale using a novel hyperbolic non-local refined plate theory is carried out by Besseghier *et al.* (2017).

In this paper, based on the proposednew model of the displacement fieldwith four variables and a warping function taking into account the effect of shear, the static behavior of FGM macro and nano-plates under thermomechanical loading using virtual work principle and local and non-local theory to determine equilibrium equations is presented.

2. Theoretical formulation

2.1 Geometrical configuration

In this study, a rectangular FG sandwich plate has dimensions "a" as length, "b" as width and "h" as thickness is considered ($a\times b\times h$). Only "Plate A" has P-FGM face sheets and an E-FGM core is studied. Its configuration is given in Fig. 1.

The median plane of the FGM sandwich plate is defined by $z=0$ and its free surfaces are defined by (the lower surface, $h_0=-h/2$) and (the upper surface, $h_3=+h/2$), the two interfaces

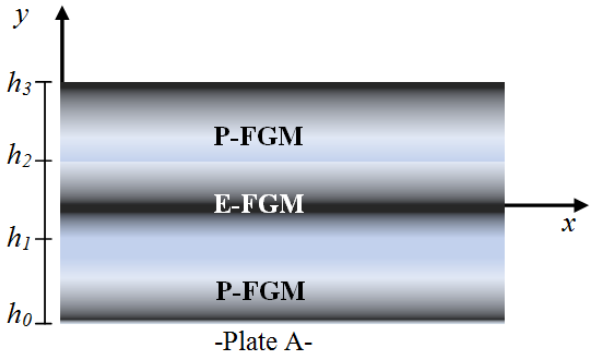

Fig. 1 Sandwich plate with FGM face sheets and FGM core

between the core and sheet faces (h_1, h_2) vary according to the configuration of the plate as:

- Sandwich plate in FGM (1-0-1): The plate is symmetrical, it consists only of two layers of FGM of the same thickness. That is, the central isotropic layer in ceramic is absent: h_1=0, h_2=0.
- Sandwich plate in FGM (1-2-1): The plate is symmetrical. The thicknesses of the central layer equal the sum of two layers (upper and lower): h_1=−h/4, h_2=+h/4.
- Sandwich plate in FGM (1-1-1): The plate is symmetrical and consists of three layers of same thicknesses: h_1=−h/6, h_2=+h/6.
- Sandwich plate in FGM (1-3-1): The plate is symmetrical. The thicknesses of the central layer equal three times upper or lower layer: h_1=−3h/10, h_2=+3h/10.
- Sandwich plate in FGM (2-1-2): The plate is symmetrical. The thickness of the central layer is half of thickness of both upper and lower layer: h_1=−h/10, h_2=+h/10.
- Sandwich plate in FGM (3-1-3): The plate is symmetrical. The thickness of the central layer is one-third of thickness of both upper and lower layer: h_1=−h/14, h_2=+h/14.

In this current investigation, the studied plate is under a thermal load varying through the thickness and a transverse mechanical load applied at the top surface.

2.2 Materials properties of the FG face sheets

The volume fraction of the FG- faces sheet are assumed varies as following relations (1) and (2) (Bensaid *et al.* 2020, Daikh *et al.* 2020a, b).

$$V^1(z) = \left(\frac{z-h_0}{h_1-h_0}\right)^p \text{ for } z \in [\![h_0, h_1]\!] \tag{1}$$

$$V^3(z) = \left(\frac{z-h_3}{h_2-h_3}\right)^p \text{ for } z \in [\![h_2, h_3]\!] \tag{2}$$

Where V^1 and V^3 are the volume fractions of the lower and upper layers, p is a material index of the faces sheets $(p \geq 0)$. The material properties (Young's modulus $E^{(n)}$, $\nu^{(n)}$ Poisson coefficient, $\alpha^{(n)}$ thermal expansion) of the two faces (lower and upper layers) at one point can be determined by the mixture law (Kettaf *et al.* 2013)

$$P^{(n)}(z) = P_m(E_c - E_m)V^{(n)} \tag{3}$$

Where *m* and *c* are index represented metal and ceramic respectively.

2.3 Materials properties of the sandwich core

The volume fraction of the sandwich core (plate A) is given by the relation

$$V^3(z) = \left(\frac{2|z|}{h_2 - h_1}\right)^{\mathrm{k}} \text{ for } \quad z \in [\![h_1, h_2]\!] \tag{4}$$

$k \geq 0$ is material index for the sandwich core (plate A). The material properties (Young's modulus $E^{(n)}$, $\nu^{(n)}$ Poisson coefficient, $\alpha^{(n)}$ thermal expansion) vary exponentially along the thickness of the layer and is expressed by the relation (5) Zenkour and Alghamdi (2010)

$$P^{(2)}(z) = P_m e^{\beta V^{(2)}} \tag{5}$$

With $\beta = ln\frac{P_c}{P_m}$

3. Kinematics and constitutive equations

3.1 Displacement fields

The displacement field of the higher order shear deformation theory is expressed by

$$u(x, y, z) = u_0(x, y) - z\,\frac{\partial w_0\,(x,y)}{\partial x} + k_1 f(z) \int \Theta\, dx \tag{6}$$

$$v(x, y, z) = v_0(x, y) - z\,\frac{\partial w_0\,(x,y)}{\partial y} + k_2\, f(z) \int \Theta\, dy \tag{7}$$

$$w(x, y, z) = w_0\,(x, y) \tag{8}$$

Where *u*, *v*, *w*, θ are displacements of the medium fiber of plate and *f*(*z*) indicates the function of the shape determining the distribution of transverse shear deformations and stresses in the direction of thickness. The function shape $f(\mathrm{z})$ is chosen as Chikh *et al*. (2017).

$$f(z) = 1 - \Psi(z) \tag{9}$$

$$\Psi(z) = \frac{2z\sin\left(\frac{z^2}{h^2}\right)}{2\sinh\left(\frac{1}{4}\right) + \cosh\left(\frac{1}{4}\right)} \tag{10}$$

The strain can be expressed by

$$\varepsilon_x(x, y, z) = \frac{\partial u_0(x,y)}{\partial x} - z\,\frac{\partial^2 w_0\,(x,y)}{\partial x^2} + k_1 f(z)\Theta \tag{11}$$

$$\varepsilon_y(x, y, z) = \frac{\partial v_0(x,y)}{\partial y} - z\,\frac{\partial^2 w_0\,(x,y)}{\partial y^2} + k_2\, f(z) \tag{12}$$

$$\begin{aligned}\gamma_{xy}(x, y, z) = &\left(\frac{\partial u_0(x,y)}{\partial y} + \frac{\partial v_0(x,y)}{\partial x}\right) - 2z\,\frac{\partial^2 w_0\,(x,y)}{\partial x \partial y} \\ &+ k_1\, f(z)\frac{\partial}{\partial y}\int \Theta dx \; + k_2\, f(z)\frac{\partial}{\partial x}\int \Theta dy\end{aligned} \tag{13}$$

$$\gamma_{yz} = k_2\, g(z) \int \Theta dy \tag{14}$$

$$\gamma_{xz} = k_1\, g(z) \int \Theta dx \tag{15}$$

The integrals used in the above equations must be solved by a Navier type solution and can be written as follows (Boussoula *et al*. 2020).

$$\frac{\partial}{\partial y}\int \Theta dx = A' \frac{\partial^2 \Theta}{\partial x \partial y},\quad \frac{\partial}{\partial x}\int \Theta dy = B' \frac{\partial^2 \Theta}{\partial x \partial y},\quad \Theta dx = A' \frac{\partial \Theta}{\partial x}, \Theta dy = B' \frac{\partial \Theta}{\partial y}\# \tag{16}$$

The coefficients *A'* and *B'* are formulated according to the Navier method and defined by

$$A' = -\frac{1}{\lambda^2}, B' = -\frac{1}{\mu^2}\ , k_1 = \lambda^2, k_2 = \mu^2 \tag{17}$$

3.2 Constitutive equations

The constitutive law takes into account the traverse shear deformation and the thermal effect of n^{th} layer: of the FG sandwich plate can be given by relation (18) and (19)

$$\begin{Bmatrix} \sigma_x \\ \sigma_y \\ \sigma_{xy} \end{Bmatrix}^n = \begin{bmatrix} c_{11}(z) & c_{12}(z) & 0 \\ c_{12}(z) & c_{22}(z) & 0 \\ 0 & 0 & c_{66}(z) \end{bmatrix}^n \begin{Bmatrix} \varepsilon_x - \alpha T \\ \varepsilon_y - \alpha T \\ \gamma_{xy} \end{Bmatrix}^n \tag{18}$$

$$\begin{Bmatrix} \gamma_{yz} \\ \gamma_{xz} \end{Bmatrix}^n = \begin{bmatrix} c_{44}(z) & 0 \\ 0 & c_{55}(z) \end{bmatrix}^n \begin{Bmatrix} \gamma_{yz} \\ \gamma_{xz} \end{Bmatrix}^n \tag{19}$$

Where n=1, 2, 3, and $(\sigma_x, \sigma_y, \sigma_{xy}, \sigma_{xz}, \sigma_{yz})$ are the components of normal and tangential stresses and $(\varepsilon_x, \varepsilon_y, \gamma_{xy}, \gamma_{xz}, \gamma_{yz})$ are the strains components.

The stiffness coefficients $C_{ij}^n(z)$ are given by the expressions (20) and (21)

$$\begin{gathered} {c_{11}}^{(n)}(z) = {c_{22}}^{(n)}(z) = \frac{E^{(n)}(z)}{1-(\nu^{(n)})^2} \\ {c_{12}}^{(n)}(z) = \nu^{(n)}\, {c_{11}}^{(n)}(z) \end{gathered} \tag{20}$$

$${c_{44}}^{(n)}(z) = {c_{55}}^{(n)}(z) = {c_{66}}^{(n)}(z) = \frac{E^{(n)}(z)}{2(1+\nu^{(n)})} \tag{21}$$

3.2 Governing equations

The equilibrium equations are determined using the principle of virtual work (Boussoula *et al*. 2020). The total potential energy for FG plates U can be expressed by

$$\begin{aligned} U = \frac{1}{2}\int_V \Big[& {\sigma_x}^{(n)}(\varepsilon_x - \alpha T)^{(n)} + {\sigma_y}^{(n)}\left(\varepsilon_y - \alpha T\right)^{(n)} \\ & + {\sigma_{xy}}^{(n)}{\gamma_{xy}}^{(n)} + {\sigma_{yz}}^{(n)}{\gamma_{yz}}^{(n)} + {\sigma_{xz}}^{(n)}{\gamma_{xz}}^{(n)}\Big] dV \end{aligned} \tag{22}$$

The principle of virtual work can be rewritten as follows

$$\int_{\Omega}\begin{bmatrix} N_{xx}\delta\varepsilon_{xx}{}^{0}+N_{yy}\delta\varepsilon_{yy}{}^{0}+N_{xy}\delta\varepsilon_{xy}{}^{0}+ \\ M_{xx}{}^{b}\delta k_{xx}{}^{b}+M_{xx}{}^{b}\delta k_{xx}{}^{b}+M_{yy}{}^{b}\delta k_{yy}{}^{b}+ \\ M_{xy}{}^{b}\delta k_{xy}{}^{b}+M_{xx}{}^{s}\delta k_{xx}{}^{s}+M_{yy}{}^{s}\delta k_{yy}{}^{s}+ \\ M_{xy}{}^{s}\delta k_{xy}{}^{s}+Q_{yz}{}^{s}\delta\gamma_{yz}{}^{s}+Q_{xz}{}^{s}\delta\gamma_{xz}{}^{s} \end{bmatrix}\mathrm{d}\Omega-\int_{\Omega} q\delta w_0 d\Omega=0 \tag{23}$$

With

$$\begin{gathered}\left(N_{ij},M^{b}{}_{ij},M^{s}{}_{ij}\right)=\sum_{\mathrm{n}=1}^{3}\int_{\mathrm{h_{n-1}}}^{\mathrm{h_n}}\left(1,\mathrm{z},\mathrm{f(z)}\right)\sigma_{\mathrm{ij}}{}^{(\mathrm{n})}dz \\ \left(Q^{s}{}_{xz},Q^{s}{}_{yz}\right)=\sum_{\mathrm{n}=1}^{3}\int_{\mathrm{h_{n-1}}}^{\mathrm{h_n}}\mathrm{g(z)}\ (\sigma_{\mathrm{xz}},\sigma_{\mathrm{yz}})^{(\mathrm{n})}\mathrm{dz}\end{gathered} \tag{24}$$

Where M, N and Q are the resultants of constraints, h_n and $h_{n\text{-}1}$ are the top and bottom coordinates of n layers. The governing equations are obtained by integrating Eqs. (23) and (24) by parts

$$\begin{gathered}\delta u_0:\frac{\partial N_{xx}}{\partial x}+\frac{\partial N_{xy}}{\partial y}=0, \\ \delta v_0:\frac{\partial N_{xy}}{\partial x}+\frac{\partial N_{yy}}{\partial y}=0, \\ \delta w_0:\frac{\partial^2 M^{b}{}_{xx}}{\partial x^2}+\frac{\partial^2 M^{b}{}_{yy}}{\partial y^2}+2\frac{\partial^2 M^{b}{}_{xy}}{\partial x\partial y}+q=0 \\ \delta\Theta:-k_1 M_{xx}{}^{s}-k_2 M_{yy}{}^{s}-(k_1A'+k_2B')\frac{\partial^2 M^{s}{}_{xy}}{\partial x\partial y}+k_1A'\frac{\partial Q^{s}{}_{xz}}{\partial x}+k_2B'\frac{\partial Q^{s}{}_{yz}}{\partial y}=0\end{gathered} \tag{25}$$

4. Nonlocal elasticity theory

In the nonlocal elasticity theory, the stress field at any point of continua body depends on the strain field at all neighboring points (Eringen 1967). For the case where the thermal effect is taken into account, the constitutive law in nonlocal elasticity is expressed by the following expression (Eringen 1972)

$$[1-(e_0l_0)^2\nabla^2]\{\sigma_{ij}\}^{(n)}=\left[C_{ij}\right]^{(n)}\{\varepsilon_{ij}-\alpha^{(n)}(z)T^{(n)}(z)\} \tag{26}$$

Where ∇^2 the Laplacian operator which is defined by: $\nabla^2=\frac{\partial^2}{\partial x^2}+\frac{\partial^2}{\partial y^2}$, α is the coefficient of thermal expansion, and $(e_0l_0)^2$ is the scale parameter.

The stress resultants can be written in contracted as follows

$$\begin{Bmatrix}\{N-(e_0l_0)^2\nabla^2N\}\\ \{M^{b}-(e_0l_0)^2\nabla^2M^{b}\}\\ \{M^{s}-(e_0l_0)^2\nabla^2M^{s}\}\end{Bmatrix}=\begin{bmatrix}\{A_{ij}\} & \{B_{ij}\} & \{C_{ij}\}\\ \{B_{ij}\} & \{D_{ij}\} & \{F_{ij}\}\\ \{C_{ij}\} & \{F_{ij}\} & \{H_{ij}\}\end{bmatrix}\begin{Bmatrix}\{\varepsilon^0\}\\ \{k^b\}\\ \{k^s\}\end{Bmatrix}-\begin{Bmatrix}\{N^T\}\\ \{M^{bT}\}\\ \{M^{sT}\}\end{Bmatrix} \tag{27}$$

$$\begin{Bmatrix}\{Q_{yz}-(e_0l_0)^2\nabla^2Q_{yz}\}\\ \{Q_{xz}-(e_0l_0)^2\nabla^2Q_{xz}\}\end{Bmatrix}=\begin{bmatrix}j_{44} & 0\\ 0 & j_{55}\end{bmatrix}\begin{Bmatrix}\gamma_{yz}\\ \gamma_{xz}\end{Bmatrix} \tag{28}$$

Where A_{ij}, B_{ij}, C_{ij}, F_{ij} and H_{ij} are the stiffness and are defined as follows by relation (29) and

(30)

$$\{A_{ij}, B_{ij}, D_{ij}, C_{ij}, F_{ij}, H_{ij}\} = \sum_{n=1}^{3} \int_{h_n-1}^{h_n} c_{ij}^{(n)} \{1, z, z^2, f(z), zf(z), f^2(z)\}\, dz \quad (29)$$

With: (i,j=1,2,6)

$$J_{ii} = \sum_{n=1}^{3} \int_{h_n-1}^{h_n} c_{ii}^{(n)} [g(z)]^2\, dz, (i = 4,5) \quad (30)$$

The stress and moment resultants $\{N^T\}$, $\{M^{bT}\}$ and $\{M^{sT}\}$ to loading thermal are defined as follows

$$\begin{matrix} \{N^T\} = \{N_x^T \quad N_y^T \quad 0\} \\ \{M^{bT}\} = \{M_x^{bT} \quad M_y^{bT} \quad 0\} \\ \{M^{sT}\} = \{M_x^{sT} \quad M_y^{sT} \quad 0\} \end{matrix} \quad (31)$$

The resultants of stresses and thermal loading moments are defined by the relation (32)

$$\begin{Bmatrix} N_x^T \\ N_y^T \end{Bmatrix} = \sum_{n=1}^{3} \int_{h_n-1}^{h_n} \begin{Bmatrix} (c_{11} + c_{12})\alpha T \\ (c_{12} + c_{22})\alpha T \end{Bmatrix}^{(n)} dz \quad (32a)$$

$$\begin{Bmatrix} M_x^{bT} \\ M_y^{bT} \end{Bmatrix} = \sum_{n=1}^{3} \int_{h_n-1}^{h_n} \begin{Bmatrix} (c_{11} + c_{12})\alpha T \\ (c_{12} + c_{22})\alpha T \end{Bmatrix}^{(n)} z\, dz \quad (32b)$$

$$\begin{Bmatrix} M_x^{sT} \\ M_y^{sT} \end{Bmatrix} = \sum_{n=1}^{3} \int_{h_n-1}^{h_n} \begin{Bmatrix} (c_{11} + c_{12})\alpha T \\ (c_{12} + c_{22})\alpha T \end{Bmatrix}^{(n)} f(z) dz \quad (32c)$$

The variation of the loading mechanical loading according to the thickness of the FGM sandwich is given by expression

$$q(x, y) = q_0 \sin(\lambda x) \sin(\mu y) \quad (33)$$

$$T(x, y, z) = T_1(x, y) + \frac{z}{h} T_2(x, y) + \frac{f(z)}{h} T_3(x, y) \quad (34)$$

Where q_0 is the mechanical loading intensity, T_1, T_2 and T_3 are linear and nonlinear thermal loading according to the thickness of the plate.

5. Analytical solution for FGM plates

In this study, we present a simply supported plate of which the boundary conditions at the four edges are defined as follows:

At $x = 0, aN_x = M_x^b = M_x^s = v_0 = w_0 = \theta = 0$

At $y = 0, bN_y = M_y^b = M_y^s = u_0 = w_0 = \theta = 0$

From Navier's solution, one can solve the problem of the thermo mechanical behavior of the sandwich plate in FGM. The displacement for the plate is written as follows (Daikh and Zenkour 2020)

$$\begin{aligned} u_0 &= U_{mn}\cos(\lambda x)\sin(\mu y) \\ v_0 &= V_{mn}\sin(\lambda x)\cos(\mu y) \\ w_0 &= W_{mn}\sin(\lambda x)\sin(\mu y) \\ \theta &= \theta_{mn}\sin(\lambda x)\sin(\mu y) \end{aligned} \tag{35}$$

Where $U_{mn}, V_{mn}, W_{mn}\ et\ \Theta_{mn}$ are arbitrary parameters represent each of the terms in the serie for Navier solution determined under the condition that the solution of equation (35). The thermal loading is presented in trigonometric form

$$T_i = t_i \sin(\lambda x)\sin(\mu y) \tag{36}$$

$i = 1,2,3$

Where $t_1, t_2 t_3$ are constants. $\lambda = \frac{\pi}{a}$, $\mu = \frac{\pi}{b}$

We obtain the operator

$$|K|\{\Delta\} = \{P\} \tag{37}$$

Where $\{\Delta\} = \{U, V, W, \Theta\}^T$ and $|K|$ is a symmetric matrix with

$$\begin{aligned} K_{11} &= A_{11}\lambda^2 + A_{66}\mu^2, K_{12} = \lambda\mu(A_{12} + A_{66}), \\ K_{12} &= \lambda\mu(A_{12} + A_{66}), \\ K_{13} &= -\lambda[B_{11}\lambda^2 + (B_{12} + 2B_{66})\mu^2], \\ K_{14} &= \lambda[k_1 A' C_{11}\lambda^2 + (k_2 B' C_{12} + (k_1 A' + k_2 B')C_{66})\mu^2], \\ K_{22} &= A_{66}\lambda^2 + A_{22}\mu^2, \\ K_{23} &= -\mu[B_{22}\mu^2 + (B_{12} + 2B_{66})\lambda^2], \\ K_{24} &= \mu[k_2 B' C_{22}\mu^2 + (k_1 A' C_{12} + (k_1 A' + k_2 B')C_{66})\lambda^2], \\ K_{33} &= D_{11}\lambda^4 + 2(D_{12} + 2D_{66})\lambda^2\mu^2 + D_{22}\mu^4 \\ K_{34} &= -k_1 A' F_{11}\lambda^4 - [(k_1 A' + k_2 B')F_{12} + 2(k_1 A' + k_2 B')F_{66}]\lambda^2\mu^2 - k_2 B' F_{22}\mu^4 \\ K_{44} &= -{k_1}^2 {A'}^2 H_{11}\lambda^4 + [(k_1 A' k_2 B')H_{12} + (k_1 A' + k_2 B')^2 H_{66}]\lambda^2\mu^2 + {k_2}^2 {B'}^2 H_{22}\mu^4 + \\ &\quad {k_1}^2 {A'}^2 J_{55}\lambda^2 + {k_2}^2 {B'}^2 J_{44}\mu^2 \end{aligned} \tag{38}$$

The components of the generalized loading $\{P\} = \{P_1, P_2, P_3, P_4\}^T$ are given as follows

$$\begin{aligned} P_1 &= -\lambda(A^T t_1 + B^T t_2 + C^T t_3) \\ P_2 &= -\mu(A^T t_1 + B^T t_2 + C^T t_3) \\ P_3 &= (1 + \lambda^2(e_0 l_0)^2 + \mu^2(e_0 l_0)^2)q_{mn} + h(\lambda^2+\mu^2)((B^T t_1 + D^T t_2 + F^T t_3) \\ P_4 &= h(\lambda^2 + \mu^2)((C^T t_1 + F^T t_2 + G^T t_3) \end{aligned} \tag{39}$$

Where

$$\{A^T, B^T, C^T\} = \sum_{n=1}^{3}\int_{h_n-1}^{h_n} \frac{E^{(n)}(z)}{1-(\nu^{(n)})^2}\left(1 + \nu^{(n)}\right)\alpha^{(n)}\{1, \bar{z}, \bar{z}^2\}\, dz \tag{40}$$

$$\{C^T, F^T, G^T\} = \sum_{n=1}^{3}\int_{h_n-1}^{h_n} \frac{E^{(n)}(z)}{1-(\nu^{(n)})^2}\left(1 + \nu^{(n)}\right)\alpha^{(n)}\bar{f}(z)\left\{1, \bar{z}, \bar{f}(z)\right\} dz \tag{41}$$

Table 1 Properties of the material

Properties	MetalTi-6Al-4V	Ceramic *ZrO2*
Young's modulus E_i (GPa)	66.2	117.0
Poisson coefficient υ_i	0.33	0.33
Thermal expansion α (10^{-6}/K)	10.3	7.11

With: $\bar{z} = \frac{z}{h}$, $\bar{f}(z) = \frac{f(z)}{h}$

6. Results and discussion

The numerical outcomes are given in terms dimensionless deflection, normal and tangential stresses. The dimensionless parameters are defined as follows

$$\bar{w} = \frac{10^3}{q_{mn}a^4/(E_0h^3) + 10^3\alpha_0 t_2 a^2/h} w\left(\frac{a}{2},\frac{b}{2}\right) \tag{42}$$

$$\overline{\sigma_x} = \frac{10}{q_{mn}a^2/h^2 + 10E_0\alpha_0 t_2 a^2/h^2} \sigma_x\left(\frac{a}{2},\frac{b}{2},z\right) \tag{43}$$

$$\overline{\tau_{xz}} = \frac{1}{q_{mn}a/h + 10E_0\alpha_0 t_2 a/(10h)} \tau_{xz}\left(0,\frac{b}{2},z\right) \tag{44}$$

With $E_0 = 1$ GPa, $\alpha_0 = 10^{-6}$/K

The material properties used in this study are shown in Table 1.

6.1 Local approach

In this first part, numerical results for local approach are presented to investigate thermo mechanical flexural response of simply supported FGM sandwich plate (Type A) using the proposal theory with four variables and a warping function taking into account the effect of shear. The results are examined and compared with those obtained by Zenkour and Alghamdi (2010) using the First Shear Deformation Theory, Li *et al.* (2017) using the refined plate theory and the theory developed by Boussoula *et al.* (2020).

In first time, bending analysis of FGM sandwich plate with face sheets and homogenous core k=0 under thermomechanical loads is studied by considering varying different parameters such power index p, different layer thickness ratios, geometry ratios and variation of the dimensionless deflection.

Table 2 presents the values of the dimensionless deflection (w) of simply supported thick square sandwich plate (a/h=10, Type A) with FGM face sheets and homogeneous core under thermo-mechanical load for several values of material index (p) and different layer thickness ratios (1-0-1, 3-1-3, 2-1-2 and 1-1-1) for various values of power index p (0,1,2,3,4,5). The results obtained are in good agreement with those obtained by Zenkour and Alghamdi (2010) , Li *et al.* (2017), Boussoula *et al.* (2020). For p=0, when the plate is entirely ceramic, the values of the dimensionless deflection are the same for all the layer thickness ratios.

Table 2 Variation of the dimensionless deflection ($\bar{w}$) square sandwich plate (a/h=10, Type A) with FGM face sheets and homogeneous core (k=0) under thermo-mechanical load for several values of power index and various values of layer thickness ratios

p	Theory	$\bar{w}\left(\frac{a}{2},\frac{b}{2}\right)$			
		1-0-1	3-1-3	2-1-2	1-1-1
0	(Zenkour and Alghamdi (2010)	0.895735	0.895735	0.895735	0.895735
	(Li *et al*. 2017)	0.864140	0.864140	0.864140	0.864140
	nth order SDT (Boussoula *et al*. 2020)	0.864140	0.864140	0.864140	0.864140
	Present	0.865438	0.865438	0.865438	0.865438
1	FSDT (Zenkour and Alghamdi 2010)	1.190728	1.170533	1.160568	1.132449
	RPT (Li *et al.* 2017)	1.149038	1.130125	1.120741	1.094113
	nthorder SDT (Boussoula *et al*. 2020)	1.149038	1.130125	1.120741	1.094113
	Present	1.151643	1.132899	1.123595	1.097162
2	FSDT (Zenkour and Alghamdi 2010)	1.257304	1.238234	1.227765	1.195703
	RPT (Li *et al.* 2017)	1.210756	1.193444	1.183826	1.154061
	nth order SDT (Boussoula *et al.* 2020)	1.210756	1.193444	1.183826	1.154061
	Present	1.213078	1.196018	1.186589	1.157163
3	FSDT (Zenkour and Alghamdi 2010)	1.280741	1.264724	1.255041	1.223232
	RPT (Li *et al.* 2017)	1.231675	1.217447	1.208690	1.179518
	nth order SDT (Boussoula *et al.* 2020)	1.231675	1.217447	1.208690	1.179518
	Present	1.233787	1.219801	1.211193	1.182506
4	FSDT (Zenkour and Alghamdi 2010)	1.290961	1.277527	1.268689	1.237931
	RPT (Li *et al.* 2017)	1.240542	1.228791	1.220879	1.192880
	nth order SDT (Boussoula *et al.* 2020)	1.240542	1.228791	1.220879	1.192880
	Present	1.242584	1.230959	1222890	1.195172
5	FSDT (Zenkour and Alghamdi 2010)	1.296101	1.284626	1.276497	1.246833
	RPT (Li *et al.* 2017)	1.244905	1.234980	1.227750	1.200876
	nth order SDT (Boussoula *et al.* 2020)	1.244905	1.234980	1.227750	1.200876
	Present	1.247118	1.239013	1.229562	1.243555

Table 3 shows the influence of the dimension ratio (a/b) on the variation of the dimensionless deflection of a square sandwich plate (type A) with two upper and lower faces in FGM and a homogeneous core (k=0) subjected to a thermo mechanical load (a/h=10, p=3) for different layer thickness ratios. It can be noted that the deflection central (w) decreases with increasing aspect ratio/a b and the lowest values lowest non-dimensional deformation are obtained for the thickness ratio layer (1-1-1). For the same thickness ratio, when p increases the stress decreases, this can be explained by the fact that the plate becomes flexible.

Table 4 present the variation of dimensionless normal stress as a function of the power index p and different layer thickness ratios for a square sandwich plate (type A) with two upper and lower faces in FGM and a homogeneous core (k=0) subjected to a thermomechanical load (a/h=10). When the thickness of the core increases the normal stress increases. The lowest values of normal stress are obtained for the FGM plate (1-0-1). When p=0, the layer thickness ratio has no effect on the dimensionless normal stress because the plate is entirely ceramic.

In this section, an analysis dimensionless deflection of sandwich plate with two faces in FGM (p=0) and an homogeneous core subjected to loads thermomechanical is considered. The variation of the dimensionless deflection as a function of the power index k and different layer thickness

Table 3 Influence of the dimension ratio (*a/b*) on the variation of the dimensionless deflection of a square sandwich plate (type A) with two upper and lower faces in FGM and a homogeneous core (*k*=0) subjected to a thermomechanical load (*a/h*=10, *p*=3) for different layer thickness ratios

Scheme	Theory	$\bar{w}\left(\frac{a}{2},\frac{b}{2}\right)$				
		a/b=1	*a/b*=2	*a/b*=3	*a/b*=4	*a/b*=5
1-0-1	FSDT (Zenkour and Alghamdi 2010)	1.280741	0.503607	0.250355	0.146917	0.095948
	RPT (Li *et al*. 2017)	1.231675	0.492573	0.246212	0.144771	0.094608
	nth order SDT (Boussoula *et al*. 2020)	1.231675	0.492573	0.246212	0.144771	0.094608
	Present	1.233787	0.493208	0.246357	0.144715	0.094455
3-1-3	FSDT (Zenkour and Alghamdi 2010)	1.264724	0.497383	0.247274	0.145112	0.094770
	RPT (Li *et al*. 2017)	1.217447	0.486952	0.243459	0.143199	0.093619
	nth order SDT (Boussoula *et al*. 2020)	1.217447	0.486952	0.243459	0.143199	0.093619
	Present	1.219801	0.487849	0.243873	0.143415	0.093735
2-1-2	FSDT (Zenkour and Alghamdi 2010)	1.255041	0.493613	0.245406	0.144017	0.094055
	RPT (Li *et al*. 2017)	1.208690	0.483486	0.241757	0.142222	0.093002
	nth order SDT (Boussoula *et al*. 2020)	1.208690	0.483486	0.241757	0.142222	0.093002
	Present	1.211193	0.484548	0.242341	0.142605	0.093288
1-1-1	FSDT (Zenkour and Alghamdi 2010)	1.223232	0.481212	0.239259	0.140414	0.091704
	RPT (Li *et al*. 2017)	1.179518	0.471920	0.236060	0.138942	0.090916
	nth order SDT (Boussoula *et al*. 2020)	1.179518	0.471920	0.236060	0.138942	0.090916
	Present	1.182506	0.473497	0.237168	0.139843	0.091714

Table 4 Variation of the dimensionless normal stress as a function of the power index *p* and different layer thickness ratios for a square sandwich plate Type A with two upper and lower faces in FGM and a homogeneous core (*k*=0) (*a/h*=10)

p	Theory	$\overline{\sigma_x}\left(a/2, b/2, h/2\right)$			
		1-0-1	3-1-3	2-1-2	1-1-1
0	FSDT (Zenkour and Alghamdi 2010)	-3 .597007	-3 .597007	-3 .597007	-3 .597007
	RPT (Li *et al*. 2017)	-2.911440	-2.911440	-2.911440	-2.911440
	nth order SDT (Boussoula *et al*. 2020)	-2.911440	-2.911440	-2.911440	-2.911440
	Present	-2.925320	-2.925320	-2.925320	-2.925320
1	FSDT (Zenkour and Alghamdi 2010)	-3.471099	-3 .569762	-3.618476	-3.756017
	RPT (Li *et al*. 2017)	-2.892290	-2.985255	-3.031378	-3.162208
	nth order SDT (Boussoula *et al*. 2020)	-2.892290	-2.985255	-3.031378	-3.162208
	Present	-2.904108	-2.997086	-3.043215	-3.174085
2	FSDT (Zenkour and Alghamdi 2010)	-3.145662	-3.238636	-3.289757	-3.446485
	RPT (Li *et al*. 2017)	-2.589234	-2.674492	-2.721838	-2.868271
	nth order SDT (Boussoula *et al*. 2020)	-2.589234	-2.674492	-2.721838	-2.868271
	Present	-2.600772	-2.685990	-2.733307	-2.879662
3	FSDT (Zenkour and Alghamdi 2010)	-3.031284	-3.109180	-3.156414	-3.311823
	RPT (Li *et al*. 2017)	-2.486287	-2.556476	-2.599635	-2.743281
	nth order SDT (Boussoula *et al*. 2020)	-2.486287	-2.556476	-2.599635	-2.743281
	Present	-2.497773	-2.567929	-2.611036	-2.754493
4	FSDT (Zenkour and Alghamdi 2010)	-2.981507	-3.046666	-3.089733	-3.239941
	RPT (Li *et al*. 2017)	-2.442566	-2.500626	-2.539661	-2.677611
	nth order SDT (Boussoula *et al*. 2020)	-2.442566	-2.500626	-2.539661	-2.677611
	Present	-2.454111	-2.512531	-2.551052	-2.691585

Table 4 Continued

5	FSDT (Zenkour and Alghamdi 2010)	-2.956534	-3 .012040	-3 .051612	-3 .196423
	RPT (Li *et al.* 2017)	-2.421017	-2.470126	-2.505817	-2.638388
	nth order SDT (Boussoula *et al.* 2020)	-2.421017	-2.470126	-2.505817	-2.638388
	Present	-2.431299	-2.470615	-2.515466	-2.707588

Table 5 Variation of the dimensionless deflection as a function of the power index *k* and different layer thickness ratios of square plate sandwich (type A) with two homogeneous upper and lower faces (*p*=0) and an FGM core (*a/h*=10)

k	Theory	$\bar{w}\left(\frac{a}{2},\frac{b}{2}\right)$			
		2-1-2	1-1-1	1-2-1	1-3-1
0	FSDT (Zenkour and Alghamdi 2010)	0.960453	0.960453	0.960453	0.960453
	RPT (Li *et al*. 2017)	0.864140	0.864140	0.864140	0.864140
	*n*th order SDT (Boussoula *et al*. 2020)	0.864140	0.864140	0.864140	0.864140
	Present	0.865438	0.865438	0.865438	0.865438
1	FSDT (Zenkour and Alghamdi 2010)	0.961067	0.963305	0.970187	0.977474
	RPT (Li *et al*. 2017)	0.864623	0.866466	0.872221	0.878396
	*n*th order SDT (Boussoula *et al*. 2020)	0.864623	0.866466	0.872221	0.878396
	Present	0.865937	0.867767	0.887704	0.879592
2	FSDT (Zenkour and Alghamdi 2010)	0.961375	0.964745	0.975191	0.986392
	RPT (Li *et al*. 2017)	0.864867	0.867635	0.876353	0.885834
	*n*th order SDT (Boussoula *et al*. 2020)	0.864867	0.867635	0.876353	0.885834
	Present	0.866185	0.868934	0.877579	0.886997
3	FSDT (Zenkour and Alghamdi 2010)	0.961565	0.965637	0.978325	0.992040
	RPT (Li *et al*. 2017)	0.865018	0.868359	0.878938	0.890547
	*n*th order SDT (Boussoula *et al*. 2020)	0.865018	0.868359	0.878938	0.890547
	Present	0.866337	0.869655	0.8801530	1.182506
4	FSDT (Zenkour and Alghamdi 2010)	0.961696	0.966250	0.980491	0.995971
	RPT (Li *et al*. 2017)	0.865121	0.868855	0.880725	0.893831
	*n*th order SDT (Boussoula *et al*. 2020)	0.865121	0.868855	0.880725	0.893831
	Present	0.866441	0.870149	0.881931	1.195172
5	FSDT (Zenkour and Alghamdi 2010)	0.961791	0.966697	0.982082	0.998875
	RPT (Li *et al*. 2017)	0.865197	0.869218	0.882038	0.896261
	*n*th order SDT (Boussoula *et al*. 2020)	0.865197	0. 869218	0.882038	0.896261
	Present	0.866517	1.239013	0.883238	1.243555

ratios of square plate sandwich (type A) with two homogeneous upper and lower faces (*p*=0) and an FGM core subjected to a thermomechanical load (*a/h*=10) is show in Table 5.

The dimensionless deflection increases very little with the material index k increases. Table 6 present the effect of the dimension ratio (*a/b*) on dimensionless of square plate square sandwich (type A) with two homogeneous upper and lower faces (*p*=0) and an FGM core subjected to a thermomechanical load (*a/h*=10, *k*=1) and for various layer thickness ratios.

It can be seen that the dimensionless arrow $\bar{w}$ decreases when the ratio a/b increases. The greatest central deflection is observed for a thickness ratio (1-3-1).

Table 7 present the variation of dimensionless normal stress as a function of the power index *k* and different layer thickness ratios of square plate square sandwich (type A) with two

Table 6 Effect of the dimension ratio (*a/b*) on dimensionless of square plate square sandwich (type A) with two homogeneous upper and lower faces (*p*=0) and an FGM core subjected to a thermomechanical load (*a/h*=10, *k*=1) and for various layer thickness ratios

Scheme	Theory	$\bar{w}\left(\frac{a}{2},\frac{b}{2}\right)$				
		a/b=1	*a/b*=2	*a/b*=3	*a/b*=4	*a/b*=5
1-2-1	FSDPT (Li *et al*. 2017)	0.970187	0.388069	0.194034	0.114137	0.074628
	RPT (Li *et al*. 2017)	0.872221	0.348604	0.174070	0.102204	0.066667
	*n*th order SDT (Boussoula *et al*. 2020)	0.872221	0.348604	0.174070	0.102204	0.066667
	Present	0.887704	0.348788	0.173920	0.101906	0.066299
1-3-1	FSDPT (Li *et al*. 2017)	0.977474	0.390984	0.195491	0.114994	0.075189
	RPT (Li *et al*. 2017)	0.878396	0.351016	0.175228	0.102846	0.067055
	*n*th order SDT (Boussoula *et al*. 2020)	0.878396	0.351016	0.175228	0.102846	0.067055
	Present	0.879592	0.375095	0.186988	0.094628	0.065457
2-1-2	FSDPT (Li *et al*. 2017)	0.961067	0.384421	0.192210	0.113064	0.073927
	RPT (Li *et al*. 2017)	0.864623	0.345661	0.172678	0.101451	0.066229
	nth order SDT (Boussoula *et al*. 2020)	0.864623	0.345661	0.172678	0.101451	0.066229
	Present	0.865937	0.345927	0.172596	0.101229	0.060922
1-1-1	FSDPT (Li *et al*. 2017)	0.963305	0.385316	0.192657	0.113328	0.074099
	RPT (Li *et al*. 2017)	0.866466	0.346369	0.173008	0.101625	0.066327
	*n*th order SDT (Boussoula *et al*. 2020)	0.866466	0.346369	0.173008	0.101625	0.066327
	Present	0.867767	0.346652	0.172908	0.101395	0.066020

Table 7 Variation of dimensionless normal stress as a function of the power index *k* and different layer thickness ratios of square plate square sandwich (type A) with two homogeneous upper and lower faces (*p*=0) and an FGM core subjected to a thermomechanical load (*a/h*=10)

k	Theory	$\overline{\sigma_x}\left(a/2, b/2, h/2\right)$			
		2-1-2	1-1-1	1-2-1	1-3-1
0	FSDPT (Li *et al*. 2017)	-4.158732	-4.158732	-4.158732	-4.158732
	RPT (Li *et al*. 2017)	-2.911440	-2.911440	-2.911440	-2.911440
	*n*th order SDT (Boussoula *et al*. 2020)	-2.911440	-2.911440	-2.911440	-2.911440
	Present	-2.925320	-2.925320	-2.925320	-2.925320
1	FSDPT (Li *et al*. 2017)	-4.153417	-4.134036	-4.074434	-4.011326
	RPT (Li *et al*. 2017)	-2.907015	-2.890699	-2.840040	-2.785860
	*n*th order SDT (Boussoula *et al*. 2020)	-2.907015	-2.890699	-2.840040	-2.785860
	Present	-2.920859	-2.904513	-2.853791	-2.799543
2	FSDPT (Li *et al*. 2017)	-4.150749	-4.121567	-4.031095	-3.934090
	RPT (Li *et al*. 2017)	-2.904809	-2.880305	-2.803535	-2.720298
	*n*th order SDT (Boussoula *et al*. 2020)	-2.904809	-2.880305	-2.803535	-2.720298
	Present	-2.918640	-2.894090	-2.817206	-2.733844
3	FSDPT (Li *et al*. 2017)	-4.149101	-4.113838	-4.003951	-3.885176
	RPT (Li *et al*. 2017)	-2.903451	-2.873883	-2.780706	-2.678783
	*n*th order SDT (Boussoula *et al*. 2020)	-2.903451	-2.873883	-2. 780706	-2. 678783
	Present	-2.917275	-2.887650	-2.794326	-2.754493
4	FSDPT (Li *et al*. 2017)	-4.147973	-4.108535	-3.985199	-3.851130
	RPT (Li *et al*. 2017)	-2.902523	-2.869484	-2.764940	-2.649867
	*n*th order SDT (Boussoula *et al*. 2020)	-2. 902523	-2. 869484	-2. 764940	-2. 649867
	Present	-2.916343	-2.883240	-2.778524	-2.663260

Table 7 Continued

5	FSDPT (Li *et al*. 2017)	-4.147150	-4.104658	-3 .971420	-3 .825981
	RPT (Li *et al*. 2017)	-2.901847	-2.866270	-2.753353	-2.628487
	*n*th order SDT (Boussoula *et al*. 2020)	-2. 901847	-2. 866270	-2. 753353	-2. 628487
	Present	-2.915664	-2.470615	-2.766911	-2.707588

Table 8 Variation of dimensionless deflection (w) as a function of the power index p and different layer thickness ratios of square sandwich plate (Type A) with P-FGM face sheets and E-FGM core under thermomechanical load (a/h=10)

p	Theory	$\bar{w}\left(\frac{a}{2},\frac{b}{2}\right)$			
		2-1-2	1-1-1	1-2-1	1-3-1
0	FSDPT (Li *et al*. 2017)	0.961067	0.963305	0.970187	0.977474
	RPT (Li *et al*. 2017)	0.864623	0.866466	0.872221	0.878396
	nth order SDT (Boussoula *et al*. 2020)	0.864623	0.866466	0.872221	0.878396
	Present	0.865937	0.867767	0.887704	0.879592
1	FSDPT (Li *et al*. 2017)	1.242779	1.217361	1.180779	1.156699
	RPT (Li *et al*. 2017)	1.121862	1.098934	1.065520	1.043229
	nth order SDT (Boussoula *et al*. 2020)	1.121862	1.098934	1.065520	1.043229
	Present	1.124665	1.101817	1.068333	1.045871
2	FSDPT (Li *et al*. 2017)	1.313230	1.284594	1.238612	1.206011
	RPT (Li *et al*. 2017)	1.185157	1.159800	1.118459	1.088746
	nth order SDT (Boussoula *et al*. 2020)	1. 185157	1.159800	1.118459	1.088746
	Present	1.187823	1.162717	1.121529	1.091729
3	FSDPT (Li *et al*. 2017)	1.341711	1.313791	1.265222	1.229142
	RPT (Li *et al*. 2017)	1.210108	1.185685	1.142459	1.109859
	nth order SDT (Boussoula *et al*. 2020)	1.210108	1185685	1.142459	1.109859
	Present	1.212578	1.188498	1.145555	1.112718
4	FSDPT (Li *et al*. 2017)	1.355934	1.329367	1.289699	1.229142
	RPT (Li *et al*. 2017)	1.222339	1.199282	1.155813	1.121864
	nth order SDT (Boussoula *et al*. 2020)	1. 222339	1.199282	1.155813	1.121864
	Present	1.224687	1.201852	1.153601	1.130099
5	FSDPT (Li *et al*. 2017)	1.364062	1.338795	1.289699	1.250973
	RPT (Li *et al*. 2017)	1.229235	1.207420	1.164203	1.129545
	nth order SDT (Boussoula *et al*. 2020)	1. 229235	1.207420	1.164203	1.129545
	Present	1.230514	1.197773	1.296510	1.034460

homogeneous upper and lower faces (p=0) and an FGM core subjected to a thermo- mechanical load (a/h=10). The stress decreases with the value of index k increase. The results obtained are close to those obtained by Boussoula *et al.* (2020), Li *et al.* (2017). On the other hand, the values obtained by the FSDT (Zenkour and Alghamdi 2010) are very high.

In the three parts, an analysis bending of sandwich plate with two faces in FGM and core in FGM (k=0) subjected to loads thermo mechanical is considered.

Table 8 shows the variation of dimensionless deflection (w) as a function of the power index pand different layer thickness ratios of square sandwich plate (Type A) with P-FGM face sheets and E-FGM core under thermo mechanical load (a/h=10). The variation of dimensionless deflection increases with the material index p. The high values are obtained for thicknessratio layer

Table 9 Effect of aspect ratio (a/b) on dimensionless deflection (w) of sandwich plate (Type A) with PFGM face sheets and E-FGM core under thermomechanical load (a/h=10, p=3, k=1)

Scheme	Theory	$\bar{w}\left(\frac{a}{2},\frac{b}{2}\right)$				
		a/b=1	a/b=2	a/b=3	a/b=4	a/b=5
2-1-2	FSDPT (Li *et al*. 2017)	1.341711	0.536675	0.268336	0.157844	0.103206
	RPT (Li *et al*. 2017)	1.210108	0.484045	0.242031	0.142378	0.093100
	*n*th order SDT (Boussoula *et al*. 2020)	1.210108	0. 484045	0. 242031	0. 142378	0.093100
	Present	1.212578	0.485069	0.242572	0.142721	0.093344
1-1-1	FSDPT (Li *et al*. 2017)	1.313791	0.525507	0.262752	0.154560	0.101058
	RPT (Li *et al*. 2017)	1.185685	0.474370	0.237271	0.139642	0.091364
	*n*th order SDT (Boussoula *et al*. 2020)	1.185685	0. 474370	0. 237271	0. 139642	0.091364
	Present	1.187823	0.475758	0.238183	0.140355	0.091976
1-2-1	FSDPT (Li *et al*. 2017)	1.265222	0.506080	0.253039	0.148846	0.097322
	RPT (Li *et al*. 2017)	1.142459	0.457190	0.228773	0.134719	0.088208
	*n*th order SDT (Boussoula *et al*. 2020)	1. 142459	0. 457190	0. 228773	0. 134719	0.088208
	Present	1.145555	0.458908	0.230029	0.135780	0.089167
1-3-1	FSDPT (Li *et al*. 2017)	1.229142	0.491649	0.245823	0.144601	0.094547
	RPT (Li *et al*. 2017)	1.109859	0.444182	0.222295	0.130929	0.085748
	*n*th order SDT (Boussoula *et al*. 2020)	1.109859	0. 444182	0. 222295	0. 130929	0.085748
	Present	1.112718	0.445877	0.223569	0.132032	0.086759

(2-1-2).

The effect of the dimension ratio (a/b) on dimensionless of square plate square sandwich (type A) with two homogeneous upper and lower faces (p=0) and an FGM core subjected to a thermo-mechanical load (a/h=10, k=1) and for various layer thickness ratios is presented in Table 9. We can noted that the dimensionless deflection (w) decrease when the aspect ratio a/b increases. Table 10 presents the variation of dimensionless normal stress as a function of the power index p and different layer thickness ratios of square plate square sandwich (type A) with P-FGM face sheets and E-FGM core under thermo mechanical load (a/h=10).

The results obtained are in good agreement and follow the same trends with those obtained by Li *et al.* (2017), Boussoula *et al.* (2020).

6.2 Nonlocal approach

In this second part, the behavior of FGM Nano plates is examined. The deflection and stresses of FG Nano plates using a four-order shear deformation theory with combination of the nonlocal strain gradient theory. The variation of dimensionless normal stress as a function of the nonlocal parameter $(e_0l_0)^2$ and different layer thickness ratios with different configurations are presented in Tables 11 to 13 and under different loading (q=100, t_1=0, t_2=t_3=100 K, q=100, t_1=t_3=0, t_2=100 K and q=100, t_1=t_3=t_2=0).

For thermomechanical loading, it can be seen that for the same layer thickness ratio, the stress values are identical, the influence of the nonlocal parameter is negligible. In the case of mechanical loading, the variation of the stress as a function of the scale parameter is very significant. We can conclude that in the case of nanoplates, the temperature does not influence the evolution of the stress.

Table 10 Variation of dimensionless normal stress as a function of the power index p and different layer thickness ratios of square plate square sandwich (type A) with P-FGM face sheets and E-FGM core (a/h=10)

p	Theory	$\overline{\sigma_x}\ (a/2,\ b/2,\ h/2)$			
		2-1-2	1-1-1	1-2-1	1-3-1
0	FSDPT (Li *et al*. 2017)	-4.153417	-4.134036	-4.074434	-4.011326
	RPT (Li *et al*. 2017)	-2.907015	-2.890699	-2.840040	-2.785860
	*n*th order SDT (Boussoula *et al*. 2020)	-2.907015	-2.890699	-2.840040	-2.785860
	Present	-2.920859	-2.904513	-2.853791	-2.799543
1	FSDPT (Li *et al*. 2017)	-4.136946	-4.261501	-4.440672	-4.558762
	RPT (Li *et al*. 2017)	-3.025929	-3.138583	-3.302462	-3.411521
	nth order SDT (Boussoula *et al*. 2020)	-3.025929	-3. 138583	-3.302462	-3.411521
	Present	-3.037798	-3.150553	-3.314721	-3.424072
2	FSDPT (Li *et al*. 2017)	-3.791718	-3.932040	-4.157364	-4.317119
	RPT (Li *et al*. 2017)	-2.715313	-2.840096	-3.043204	-3.188866
	*n*th order SDT (Boussoula *et al*. 2020)	-2. 715313	-2. 840096	-3.043204	-3.188866
	Present	-2.726809	-2.851587	-3.054872	-3.200811
3	FSDPT (Li *et al*. 2017)	-3.652156	-3.788971	-4.026970	-4.203773
	RPT (Li *et al*. 2017)	-2.592638	-2.712947	-2.925506	-3.085463
	*n*th order SDT (Boussoula *et al*. 2020)	-2. 592638	-2.712947	-2. 925506	-3.085463
	Present	-2.604054	-2.724223	-2.936901	-3.098048
4	FSDPT (Li *et al*. 2017)	-3.582456	-3.712645	-3.953554	-4.138716
	RPT (Li *et al*. 2017)	-2.532421	-2.646085	-2.859957	-3.026620
	*n*th order SDT (Boussoula *et al*. 2020)	-2.532421	-2. 646085	-2. 859957	-3.026620
	Present	-2.543889	-2.654959	-2.887632	-3.037757
5	FSDPT (Li *et al*. 2017)	-4.153417	-4.134036	-4.074434	-4.011326
	RPT (Li *et al*. 2017)	-2.907015	-2.890699	-2.840040	-2.785860
	*n*th order SDT (Boussoula *et al*. 2020)	-2.907015	-2.890699	-2.840040	-2.785860
	Present	-2.920859	-2.904513	-2.853791	-2.799543

Table 11 Variation of normal stress as a function of the nonlocal parameter $(e_0l_0)^2$ and different layer thickness ratios of square nanoplate sandwich (type A) with P-FGM face sheets and ahomogeneous core under mechanical and thermal loading (P=3, k=0)

Loading	$(e_0l_0)^2$	$\overline{\sigma_x}\ (a/2,\ b/2,\ h/2)$			
		1-0-1	3-1-3	2-1-2	1-1-1
q=100 t_1=0 t_2=t_3=100	0	-2.497773	-2.567929	-2.611036	-2.754493
	0.5	-2.497766	-2.567917	-2.611026	-2.754478
	1	-2.497736	-2.567888	-2.610997	-2.754451
	1.5	-2.497687	-2.567839	-2.610949	-2.754404
	2	-2.497618	-2.567771	-2.610882	-2.754340
q=100 t_1=t_3=0 t_2=100	0	-1.764135	-1.804735	-1.829437	-1.910932
	0.5	-1.764126	-1.804725	-1.829427	-1.910923
	1	-1.764096	-1.804725	-1.829398	-1.910895
	1.5	-1.764046	-1.804696	-1.829350	-1.910849
	2	-1.763977	-1.804580	-1.829283	-1.917784
q=100 t_1=t_2=t_3=0	0	2.007284	1.967091	1.944276	1.872672
	0.5	2.106340	2.064163	2.040222	1 .965085
	1	2.403507	2.355380	2.328061	2.242323
	1.5	2.898784	2.840740	2.807792	2.704386
	2	3.592173	3.520245	3.479415	3.351275

Table 12 Variation of dimensionless normal stress as a function of the nonlocal parameter (e_0l_0) and different layer thickness ratios of square nanoplate sandwich (type A) with two homogeneous upper and lower faces (p=0) and E-FGM core (k=1) under mechanical and thermal loading

Loading	$(e_0l_0)^2$	$\overline{\sigma_x}(a/2,b/2,h/2)$			
		2-1-2	1-1-1	1-2-1	1-3-1
	0	-2.920859	-2.904513	-2.853791	-2.799543
q=100	0.5	-2.920848	-2.904503	-2.853780	-2.799532
t_1=0	1	-2.920818	-2.904472	-2.853749	-2.799501
t_2=t_3=100	1.5	-2.920766	-2.904420	-2.853697	-2.799448
	2	-2.920694	-2.904348	-2.853624	-2 .799374
	0	-2.076618	-2.066984	-2.037332	-2.005906
q=100	0.5	-2.076608	-2.066974	-2.037322	-2.005896
t_1=t_3=0	1	-2.076577	-2.066943	-2.037291	-2.005864
t_2=100	1.5	-2.076526	-2.066892	-2.037239	-2.005811
	2	-2.076454	-2.066819	-2.037166	-2.005738
	0	2.082656	2.089908	2.112409	2.136467
q=100	0.5	2.185431	2.193041	2.216652	2.241898
	1	2.493756	2.502439	2.529382	2.558189
t_1=t_2=t_3=0	1.5	3.007631	3.018104	3.050598	3.085341
	2	3.727056	3.740033	3.780303	3.823354

Table 13 Variation of dimensionless normal stress as a function of the nonlocal parameter $(e_0l_0)^2$and different layer thickness ratios of square nanoplate sandwich (type A) with P-FGM facesheets (P=3) and E-FGM core (k=1) under mechanical and thermal loading (a/h=10)

Loading	$(e_0l_0)^2$	$\overline{\sigma_x}(a/2,b/2,h/2)$			
		2-1-2	1-1-1	1-2-1	1-3-1
	0	-2.604054	-2.724223	-2.936901	-3.098086
q=100	0.5	-2.604048	-2.724219	-2.936887	-3.098078
t_1=0	1	-2.604019	-2.724191	-2.936861	-3.098052
t_2=t_3=100	1.5	-2.603904	-2.724145	-2.936817	-3.098010
	2	-2.603904	-2.724080	-2.936755	-3.097951
	0	-1.825423	-1.893572	-2.012302	-2.100635
q=100	0.5	-1.825414	-1.893562	-2.012293	-2.100627
t_1=t_3=0	1	-1.825385	-1.893534	-2.012266	-2.100601
t_2=100	1.5	-1.825337	-1.893488	-2.012222	-2.100559
	2	-1.825270	-1.893423	-2.012161	-2.100500
	0	1.947311	1.885790	1.783385	1.709041
q=100	0.5	2.043407	1.978850	1.871392	1.793379
	1	2.331694	2.258031	2.135412	2.046393
t_1=t_2=t_3=0	1.5	2.812174	2.723331	2.575444	2.468082
	2	3.484846	3.374751	3.191490	3.058447

Concerning the non-local approach, under thermomechanical loading the effect of nonlocal parameter is negligible, for the same layer thickness ratio, the stress values are identical. In case of mechanical loading, the variation of the stress as a function of the scale parameter is very significant. The temperature has not influence the evolution of the stress in the case of nano plates.

Figs. 2 to 4 show the variation of deflection ratio between nonlocal and local deflection as a

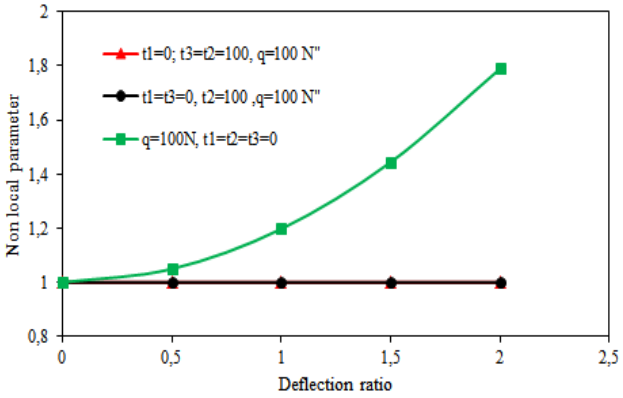

Fig. 2 Variation of deflection ration as a function of the nonlocal parameter $(e_0l_0)^2$ and different layer thickness ratios of square nanoplate sandwich (type A) with P-FGM face sheets (P=3) and homogeneous core (k=0) under mechanical and thermal loading

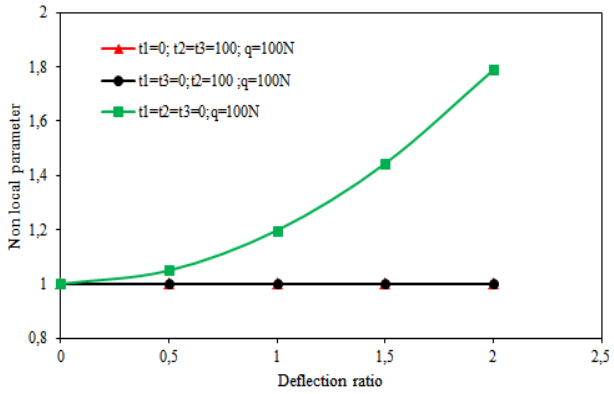

Fig. 3 Variation of the deflection ratio as a function of the nonlocal parameter $(e_0l_0)^2$ and different layer thickness ratios of square nanoplate sandwich (type A) with two homogeneous upper and lower faces (p=0) and E-FGM core (k=1) under mechanical and thermal loading

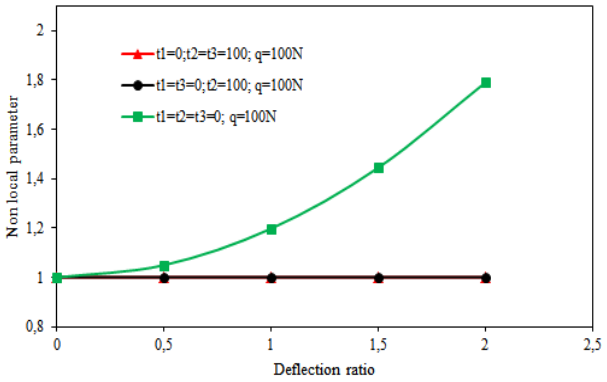

Fig. 4 Variation of the deflection ratio as a function of the nonlocal parameter $(e_0l_0)^2$ and different layer thickness ratios of square nanoplate sandwich (type A) with P-FGM face sheets and E-FGM core under mechanical and thermal loading (P=3, k=1) (a/h=10)

function of the nonlocal parameter $(e_0l_0)^2$ for square nanoplate sandwich (type A) respectively with P-FGM face sheets (P=3) and a homogeneous core (k=0), two homogeneous upper and lower faces (p=0) and E-FGM core (k=1) and P-FGM face sheets (p=3) and E-FGM core (k=1) under mechanical and thermal loading. We can note that thermomechanical does not influence the evolution of the deflection ratio.

6. Conclusions

In the present work the static analyses of FGM macro and nano-plates under thermomechanical loading has been investigated by utilizing a theory with a new displacement field with four variables and a warping function taking into account the effect of shear. The equilibrium equations deduced by using the virtual work principle and local and non-local theory, and then are solved by the Navier method with boundary conditions of plate simply supported.

- The current model is using a new displacement field with four variables and a warping function considering the effect of shear
- The results obtained are in good agreement with those obtained by the theory of the plates refined in order to validate the precision of the present theory.
- The dimensionless deflection increases with the material index k increases.
- The dimensionless arrow $\overline{w}$ decreases when the ratio a/b increases.
- The stress decreases with the value of index k increase

References

Abbas, S., Benguediab, S., Draiche, K., Bakora, A. and Benguediab, M. (2020), "An efficient shear deformation theory with stretching effect for bending stress analysis of laminated composite plates", *Struct. Eng. Mech.*, **74**(3), 365-380. https://doi.org/10.12989/sem.2020.74.3.001.

Abdelrahman, A.A., Esen, I. and Eltaher, M.A. (2021c), "Vibration response of Timoshenko perforated microbeams under accelerating load and thermal environment", *Appl. Math. Comput.*, **407**, 126307. https://doi.org/10.1016/j.amc.2021.126307.

Abdelrahman, A.A., Esen, I., Özarpa, C. and Eltaher, M.A. (2021a), "Dynamics of perforated nanobeams subject to moving mass using the nonlocal strain gradient theory", *Appl. Math. Model.*, **96**, 215-235. https://doi.org/10.1016/j.apm.2021.03.008.

Abdelrahman, A.A., Esen, I., Ozarpa, C., Shaltout, R., Eltaher, M.A. andAssie, A.E. (2021b), "Dynamics of perforated higher order nanobeams subject to moving load using the nonlocal strain gradient theory", *Smart Struct. Syst.*, **28**(4), 515-533. https://doi.org/10.12989/sss.2021.28.4.515.

Aifantis, E.C. (1999), "Gradient deformation models at nano, micro, and macro scales", *J. Eng. Mater. Technol.-Trans.*, ASME, **121**(2), 189-202. https://doi.org/10.1115/1.2812366.

Alazwari, M.A., Eltaher, M.A. and Abdelrahman, A.A. (2022a), "On bending of cutout nanobeams based on nonlocal strain gradient elasticity theory", *Steel Compos. Struct.*, **43**(6), 707-723. https://doi.org/10.12989/scs.2022.43.6.707.

Alazwari, M.A., Essen, I., Abdraboh, M.A., Abdelrahman, A.A. and Eltaher, M.A. (2022b), "Dynamic analysis of functionally graded (FG) nonlocal strain gradient nanobeams under thermo-magnetic fields and moving load", *Adv. Nano Res.*, **12**(3), 231-251. https://doi.org/10.12989/anr.2022.12.3.231.

Ameur M., Tounsi A., Mechab I. and Adda Bedia E.A. (2011), "A new trigonometric shear deformation theory for bending analysis of functionally graded plates resting on elastic foundations", *KSCE J. Civil Eng.*, **15**(8), 1405-1414. https://doi.org/10.1007/s12205-011-1361-z.

Assie, A.E., Mohamed, S.M., Shanab, R.A., Abo-bakr, R.M. and Eltaher, M.A. (2023), "Static buckling of 2D FG porous plates resting on elastic foundation based on unified shear theories", *J. Appl. Comput. Mech.*, **9**(1), 239-258. https://doi.org/10.22055/jacm.2022.41265.3723.

Attia, M.A., Melaibari, A., Shanab, R.A. and Eltaher, M.A. (2022), "Dynamic analysis of sigmoid bidirectional FG microbeams under moving load and thermal load: Analytical laplace solution", *Math.*, **10**(24), 4797. https://doi.org/10.3390/math10244797.

Belabed, Z., Bousahla, A.A., Houari, M.S.A., Tounsi, A. and Mahmoud, S.R. (2018), "A new 3-unknown hyperbolic shear deformation theory for vibration of functionally graded sandwich plate", *Earthq. Struct.*, **14**(2), 103-115. https://doi.org/10.12989/eas.2018.14.2.103.

Belkorissat, I., Houari, M.S.A., Tounsi, A., Adda Bedia, E.A. and Mahmoud, S.R. (2015), "On vibration properties of functionally graded nano-plate using a new nonlocal refined four variable model", *Steel Compos. Struct.*, **18**(4), 1063-1081. https://doi.org/10.12989/scs.2015.18.4.1063.

Bellifa, H., Benrahou, K.H., Bousahla, A.A., Tounsi, A. and Mahmoud, S.R. (2017b), "A nonlocal zeroth-order shear deformation theory for nonlinear postbuckling of nanobeams", *Struct. Eng. Mech.*, **62**(6), 695-702. https://doi.org/10.12989/sem.2017.62.6.695.

Bellifa, H., Benrahou, K.H., Hadji, L., Houari, M.S.A. and Tounsi, A. (2016), "Bending and free vibration analysis of functionally graded plates using a simple shear deformation theory and the concept the neutral surface position", *J. Brazil. Soc. Mech. Sci. Eng.*, **38**(1), 265-275. https://doi.org/10.1007/s40430-015-0354-0.

Bensaid, I., Daikh, A.A. and Drai, A. (2020), "Size-dependent free vibration and buckling analysis of sigmoid and power law functionally graded sandwich nanobeams with microstructural defects", *J. Mech. Eng. Sci.*, **234**(18), 3667-3688. https://doi.org/10.1177/0954406220916481.

Besseghier, A., Heireche, H., Bousahla, A.A., Tounsi, A. and Benzair, A. (2015), "Nonlinear vibration properties of a zigzag single-walled carbon nanotube embedded in a polymer matrix", *Adv. Nano Res.*, **3**(1), 29-37. http://doi.org/10.12989/anr.2015.3.1.029.

Besseghier, A., Houari, M.S.A., Tounsi, A. and Mahmoud, S.R. (2017), "Free vibration analysis of embedded nanosize FG plates using a new nonlocal trigonometric shear deformation theory", *Smart Struct. Syst.*, **19**(6), 601-614. https://doi.org/10.12989/sss.2017.19.6.601.

Boussoula, A., Boucham, B., Bourada, M., Bourada, F., Tounsi, A., Bousahla, A.A. and Tounsi, A. (2020), "A simple nth-order shear deformation theory for thermomechanical bending analysis of different configurations of FG sandwich plates", *Smart Struct. Syst.*, **25**(2), 197-218. https://doi.org/10.12989/sss.2020.25.2.197.

Chikh, A., Tounsi, A., Hebali, H. and Mahmoud, S.R. (2017), "Thermal buckling analysis of cross-ply laminated plates using a simplified HSDT", *Smart Struct. Syst.*, **19**(3), 289-297. https://doi.org/10.12989/sss.2017.19.3.289.

Daikh, A., Bensaid, I. and Zenkour, A.M. (2020), "Temperature dependent thermomechanical bending response of functionally graded sandwich plates", *Eng. Res. Expr.*, **2**(1), 015006. https://doi.org/10.1088/2631-8695/ab638c.

Daikh, A., Guerroudj, M., El Adjrami, M. and Megueni, A. (2020). "Thermal buckling of functionally graded sandwich beams", *Adv. Mater. Res.*, **1156**, 43-59. https://doi.org/10.4028/www.scientific.net/amr.1156.43.

Daikh, A.A. and Zenkour, A. (2020), "Bending of functionally graded sandwich nanoplates resting on pasternak foundation under different boundary conditions", *J. Appl. Comput. Mech.*, **6**, 1245-1259. https://doi.org/10.22055/jacm.2020.33136.2166.

Daikh, A.A., Houari, M.S.A. and Eltaher, M.A. (2021), "A novel nonlocal strain gradient Quasi-3D bending analysis of sigmoid functionally graded sandwich nanoplates", *Compos. Struct.*, **262**, 113347. https://doi.org/10.1016/j.compstruct.2020.113347.

Dastjerdi, S. and Akgöz. B. (2018), "New static and dynamic analyses of macro and nano FGM plates using exact three-dimensional elasticity in thermal environment", *Compos. Struct.*, **192**, 626-641. https://doi.org/0.1016/j.compstruct.2018.03.058.

Dean, J., Fallah, A.S., Brown, P.M., Louca, L.A. and Clyne, T.W. (2011), "Energy absorption during

projectile perforation of lightweight sandwich panels with metallic fibre cores", *Compos. Struct.*, **93**(3), 1089-1095. https://doi.org/10.1016/j.compstruct.2010.09.019.

Eltaher, M.A. and Mohamed, S.A. (2020), "Buckling and stability analysis of sandwich beams subjected to varying axial loads", *Steel Compos. Struct.*, **34**(2), 241-260. https://doi.org/10.12989/scs.2020.34.2.241.

Eltaher, M.A., Abdraboh, A.M. and Almitani, K.H. (2018), "Resonance frequencies of size dependent perforated nonlocal nanobeam", *Microsyst. Technol.*, **24**(9), 3925-3937. https://doi.org/10.1007/s00542-018-3910-6.

Eltaher, M.A., Khater, M.E. and Emam, S.A. (2016), "A review on nonlocal elastic models for bending, buckling, vibrations, and wave propagation of nanoscale beams", *Appl. Math. Model.*, **40**(5-6), 4109-4128. https://doi.org/10.1016/j.apm.2015.11.026.

Eltaher, M.A., Wagih, A., Melaibari, A., Alsoruji, G.S. and Attia, M.A. (2022), "Elastoplastic indentation response of sigmoid/power functionally graded ceramics structures", *Polym.*, **14**(6), 1225. https://doi.org/10.3390/polym14061225.

Eringen, A.C. (1967), "Theory of micropolar plates", *J. Appl. Math. Phys.*, **18**, 12-30. https://doi.org/10.1007/BF01593891.

Eringen, A.C. (1972), "Nonlocal polar elastic continua", *Int. J. Eng. Sci.*, **10**, 1-16. https://doi.org/10.1016/0020-7225(72)90070-5.

Esen, I., Abdelrhmaan, A.A. and Eltaher, M.A. (2022a), "Free vibration and buckling stability of FG nanobeams exposed to magnetic and thermal fields", *Eng. Comput.*, **38**, 3463-3482. https://doi.org/10.1007/s00366-021-01389-5.

Esen, I., Alazwari, M.A., Eltaher, M.A. and Abdelrahman M.A. (2022b), "Dynamic response of FG porous nanobeams subjected thermal and magnetic fields under moving load", *Steel Compos. Struct.*, **42**(6), 805-826. https://doi.org/10.12989/scs.2022.42.6.805.

Esen, I., Özarpa, C. and Eltaher, M.A. (2021), "Free vibration of a cracked FG microbeam embedded in an elastic matrix and exposed to magnetic field in a thermal environment", *Compos. Struct.*, **261**, 113552. https://doi.org/10.1016/j.compstruct.2021.113552.

Ghandourah, E.E., Daikh, A.A., Alhawsawi, A.M., Fallatah, O.A. and Eltaher, M.A. (2022), "Bending and buckling of FG-GRNC laminated plates via quasi-3D nonlocal strain gradient theory", *Math.*, **10**(8), 1321. https://doi.org/10.3390/math10081321.

Hamed, M.A., Eltaher, M.A., Sadoun, A.M. and Almitani, K.H. (2016), "Free vibration of symmetric and sigmoid functionally graded nanobeams", *Appl. Phys. A*, **122**(9), 1-11. https://doi.org/10.1007/s00339-016-0324-0.

Hamed, M.A., Mohamed, S.A. and Eltaher, M.A. (2020), "Buckling analysis of sandwich beam rested on elastic foundation and subjected to varying axial in-plane loads", *Steel Compos. Struct.*, **34**(1), 75-89. https://doi.org/10.12989/scs.2020.34.1.075.

Hendi, A., Eltaher, M.A., Mohamed, S.A., Attia, M.A. and Abdalla, A.W. (2021), "Nonlinear thermal vibration of pre/post-buckled two-dimensional FGM tapered microbeams based on a higher order shear deformation theory", *Steel Compos. Struct.*, **41**(6), 787-803. https://doi.org/10.12989/scs.2021.41.6.787.

Javaheri, R. and Eslami, M.R. (2002), "Buckling of functionally graded plates under in-plane compressive loading", *J. Appl. Math. Mech.*, **82**, 277-283. https://doi.org/10.1002/1521-4001(200204)82:4<277::AID-ZAMM277>3.0.CO;2-Y.

Karama, M., Afaq, K.S. and Mistou, S. (2003), "Mechanical behaviour of laminated composite beam by the new multilayered laminated composite structures model with transverse shear stress continuity", *Int. J. Solid. Struct.*, **40**(6), 1525-1546. https://doi.org/10.1016/S0020-7683(02)00647-9.

Karamanli, A., Eltaher, M.A., Thai, S. and Vo, T.P. (2023), "Transient dynamics of 2D-FG porous microplates under moving loads using higher order finite element model", *Eng. Struct.*, **278**, 115566. https://doi.org/10.1016/j.engstruct.2022.115566.

Kettaf, F.Z., Houari, M.S.A., Benguediab, M. and Tounsi, A. (2013), "Thermal buckling of functionally graded sandwich plates using a new hyperbolic shear displacement model", *Steel Compos. Struct.*, **15**(4), 399-423. https://doi.org/10.12989/scs.2013.15.4.399.

Kirchhoff, G.R. (1850), "Uber das gleichgewicht und die bewegungeiner elastischen scheibe", *J. Reine*

Angew. Math., **40**, 51-88.
Li, D., Deng, Z. and Xiao, H. (2016), "Thermomechanical bending analysis of functionally graded sandwich plates using four variable refined plate theory", *Compos. Part B-Eng.*, **106**, 107-119. https://doi.org/10.1016/j.compositesb.2016.08.041.
Li, D., Deng, Z., Chen, G., Xiao, H. and Zhu, L. (2017), "Thermomechanical bending analysis of sandwich plates with both functionally graded face sheets and functionally graded core", *Compos. Struct*., **169**, 29-41. http://doi.org/10.1016/j.compstruct.2017.01.026.
Librescu, L. and Hause, T. (2000), "Recent developments in the modeling and behavior of advanced sandwich constructions: A survey", *Compos*. *Struct*., **48**(1-3), 1-17. https://doi.org/10.1016/S0263-8223(99)00068-9.
Lindström, A. and Hallström, S. (2010), "Energy absorption of SMC/balsa sandwich panels with geometrical triggering features", *Compos*. *Struct*., **92**(11), 2676-2684. https://doi.org/10.1016/j.compstruct.2010.03.018.
Mahi, A., Adda Bedia, E.A. and Tounsi, A. (2015), "A new hyperbolic shear deformation theory for bending and free vibration analysis of isotropic, functionally graded, sandwich and laminated composite plates", *Appl*. *Math*. *Model*., **39**(9), 2489- 2508. https://doi.org/10.1016/j.apm.2014.10.045.
Malhari Ramteke, P., Kumar Panda, S. and Sharma, N. (2022), "Nonlinear vibration analysis of multidirectional porous functionally graded panel under thermal environment", *AIAA J.*, **60**(8), 4923-4933. https://doi.org/10.2514/1.J061635.
Mantari, J.L. (2015), "A refined theory with stretching effect for the dynamics analysis of advanced composites on elastic foundation", *Mech. Mater*., **86**, 31-43. https://doi.org/10.1016/j.mechmat.2015.02.010.
Melaibari, A., Mohamed, S.A., Assie, A.E., Shanab, R.A. and Eltaher, M.A. (2023), "Mathematical and physical analyses of middle/neutral surfaces formulations for static response of bi-directional FG plates with movable/immovable boundary conditions", *Math.*, **11**(1), 2. https://doi.org/10.3390/math11010002.
Melaibari, A., Mohamed, S.A., Assie, A.E., Shanab, R.A. and Eltaher, M.A. (2022), "Static response of 2D FG porous plates resting on elastic foundation using midplane and neutral surfaces with movable constraints", *Math.*, **10**(24), 4784. https://doi.org/10.3390/math10244784.
Merdaci, S., Tounsi, A., Houari, M.S.A., Mechab, I., Hebali, H. and Benyoucef, S. (2011), "Two new refined shear displacement models for functionally graded sandwich plates", *Arch. Appl. Mech*., **81**(11), 1507-1522. https://doi.org/10.1007/s00419-010-0497-5.
Mindlin, R.D. (1951), "Influence of rotary inertia and schear on flexural motions of isotropic, elastic plates", *J. Appl. Mech.*, **18**, 31-38. https://doi.org/10.1115/1.4010217.
Mohamed, S., Assie, A.E., Mohamed, N. and Eltaher, M.A. (2022), "Static and stress analyses of bi-directional FG porous plate using unified higher order kinematics theories", *Steel Compos. Struct*., **45**(3), 305-330. https://doi.org/10.12989/scs.2022.45.3.305.
Nguyen, T.K., Sab, K. and Bonnet, G. (2008), "First-order shear deformation plate models for functionally graded materials", *Compos. Struct*., **83**(1), 25-36. https://doi.org/10.1016/j.compstruct.2007.03.004.
Ramteke, P.M. (2019), "Effect of grading pattern and porosity on the eigen characteristics of porous functionally graded structure", *Steel Compos. Struct*., **33**(6), 865-875. https://doi.org/10.12989/scs.2019.33.6.865.
Ramteke, P.M. and Panda, S.K. (2021b), "Free vibrational behaviour of multi-directional porous functionally graded structures", *Arab. J. Sci. Eng.*, **46**(8), 7741-7756. https://doi.org/10.1007/s13369-021-05461-6.
Ramteke, P.M., Kumar, V., Sharma, N. and Panda, S.K. (2022c), "Geometrical nonlinear numerical frequency prediction of porous functionally graded shell panel under thermal environment", *Int. J. Nonlin. Mech.*, **143**, 104041. https://doi.org/10.1016/j.ijnonlinmec.2022.104041.
Ramteke, P.M., Mahapatra, B.P., Panda, S.K. and Sharma, N. (2020a), "Static deflection simulation study of 2D functionally graded porous structure", *Mater. Today: Proc.*, **33**, 5544-5547. https://doi.org/10.1016/j.matpr.2020.03.537.
Ramteke, P.M., Mehar, K., Sharma, N. and Panda, S.K. (2021a), "Numerical prediction of deflection and stress responses of functionally graded structure for grading patterns (power-law, sigmoid, and

exponential) and variable porosity (even/uneven)", *Scientia Iranica*, **28**(2), 811-829.
Ramteke, P.M., Panda, S.K. and Patel, B. (2022a), "Nonlinear eigenfrequency characteristics of multi-directional functionally graded porous panels", *Compos. Struct*., **279**, 114707. https://doi.org/10.1016/j.compstruct.2021.114707.
Ramteke, P.M., Patel, B. and Panda, S.K. (2020b), "Time-dependent deflection responses of porous FGM structure including pattern and porosity", *Int. J. Appl. Mech.*, **12**(09), 2050102. https://doi.org/10.1142/S1758825120501021.
Ramteke, P.M., Patel, B. and Panda, S.K. (2021c), "Nonlinear eigenfrequency prediction of functionally graded porous structure with different grading patterns", *Wave. Random Complex Media*, 1-19. https://doi.org/10.1080/17455030.2021.2005850.
Ramteke, P.M., Sharma, N., Choudhary, J., Hissaria, P. and Panda, S.K. (2022b), "Multidirectional grading influence on static/dynamic deflection and stress responses of porous FG panel structure: A micromechanical approach", *Eng. Comput.*, **38**(4), 3077-3097. https://doi.org/10.1007/s00366-021-01449-w.
Reddy, J.N. (1997), *Mechanics of Laminated Composites Plates: Theory and Analysis*, CRC Press, Boca Raton.
Reddy, J.N. and Cheng, Z.Q. (2001), "Three-dimensional thermomechanical deformations of functionally graded rectangular plates", *Eur. J. Mech. A Solid*., **20**(5), 841-855. https://doi.org/10.1016/S0997-7538(01)01174-3.
Reissner, E. (1945), "The effect of transverse shears deformation on the bending of elastic plates", *J. Appl. Mech*., **12**, 69-77. https://doi.org/10.1115/1.4009435.
Sekkal, M., Fahsi, B., Tounsi, A. and Mahmoud, S.R. (2017b), "A new quasi-3D HSDT for buckling and vibration of FG plate", *Struct*. *Eng*. *Mech*., **64**(6), 737-749. https://doi.org/10.12989/sem.2017.64.6.737.
Shimpi, R.P. (2002), "Refined plate theory and its variants", *AIAA J.*, **40**(1) 137-146. https://doi.org/10.2514/2.1622.
Tounsi, A., Houari, M.S.A., Benyoucef, S. and Adda Bedia, E.A. (2013), "A refined trigonometric shear deformation theory for thermoelastic bending of functionally graded sandwich plates", *Aerosp. Sci. Technol*., **24**, 209-220. https://doi.org/10.1016/j.ast.2011.11.009.
Touratier, M. (1991), "An efficient standard plate theory", *Int. J. Eng. Sci.*, **29**(8), 901-916. https://doi.org/10.1016/0020-7225(91)90165-Y.
Xiang, S., Wang, K.M., Ai, Y.T., Sha, Y.D. and Shi, H. (2009), "Analysis of isotropic, sandwich and laminated plates by a meshless method and various shear deformation theories", *Compos. Struct.*, **91**(1), 31-37. https://doi.org/10.1016/j.compstruct.2009.04.029.
Yahia, S.A., Atmane, H.A., Houari, M.S.A. and Tounsi, A. (2015), "Wave propagation in functionally graded plates with porosities using various higher-order shear deformation plate theories", *Struct. Eng. Mech.*, **53**(6), 1143-1165. https://doi.org/10.12989/sem.2015.53.6.1143.
Zenkour, A. and Alghamdi, N.A. (2010), "Bending analysis of functionally graded sandwich plates under the effect of mechanical and thermal loads", *Mech*. *Adv*. *Mater*. *Struct*., **17**(6), 419-432. https://doi.org/10.1080/15376494.2010.483323.
Zenkour, A. and Abouelregal, A.E. (2015), "Nonlocal thermoelastic nanobeam subjected to a sinusoidal pulse heating and temperature-dependent physical properties", *Microsyst. Technol.*, **21**(8), 1767-1776. https://doi.org/10.1007/s00542-014-2294-5.
Zhao, X., Lee, Y.Y. and Liew, K.M. (2009), "Free vibration analysis of functionally graded plates using the element-free kp-Ritz method", *J. Sound Vib*., **319**(3-5), 918-939. https://doi.org/10.1016/j.jsv.2008.06.025.
Zidi, M., Tounsi, A., Houari, M.S.A., Adda Bedia, E.A. and Anwar Bég, O. (2014), "Bending analysis of FGM plates under hygrothermo-mechanical loading using a four variable refined plate theory", *Aerosp. Sci*. *Technol*., **34**, 24-34. https://doi.org/10.1016/j.ast.2014.02.001.
Zine, A., Tounsi, A., Draiche, K., Sekkal, M. and Mahmoud, S.R. (2018), "A novel higher-order shear deformation theory for bending and free vibration analysis of isotropic and multilayered plates and shells", *Steel Compos*. *Struct*., **26**(2), 125-137. https://doi.org/10.12989/scs.2018.26.2.125.